Oil-impregnated paper bushing insulation diagnostics

Special application of Dielectric Frequency Response measurements

ABSTRACT

As reported in CIGRE TB 642, windings, tap changers and bushing related failures are the major contributors to transformer failure. About 17 % of transformer breakdowns are caused by bushing failure which is often followed by explosion, tank rupture, fire and potential human harm. To date, the insulation system in high voltage and extra-high voltage bushings is mainly oil-impregnated paper and resin-impregnated paper; in fewer cases, resin-bonded paper. Some of the advantages of using oil-impregnated paper bushings, listed in CIGRE TB 445, are the ability to be used at any voltage design level with minimum partial discharge activity, relative low cost, the possibility to perform non-intrusive dielectric diagnosis using dielectric response methods, as well as the extraction of oil samples for dissolved gas analysis. Evidencing these advantages, a combined analysis of the insulation condition of EHV bushings using dielectric frequency response measurements and dissolved gas analysis are carried out at a major North American utility and are described herein.

KEYWORDS

high voltage bushing, oil-impregnated paper insulation, dielectric frequency response, DGA

Diego M. ROBALINO, Ismail GÜNER, Peter WERELIUS

Transformer breakdowns caused by bushing failure are often followed by explosion, tank rupture, fire and potential human harm

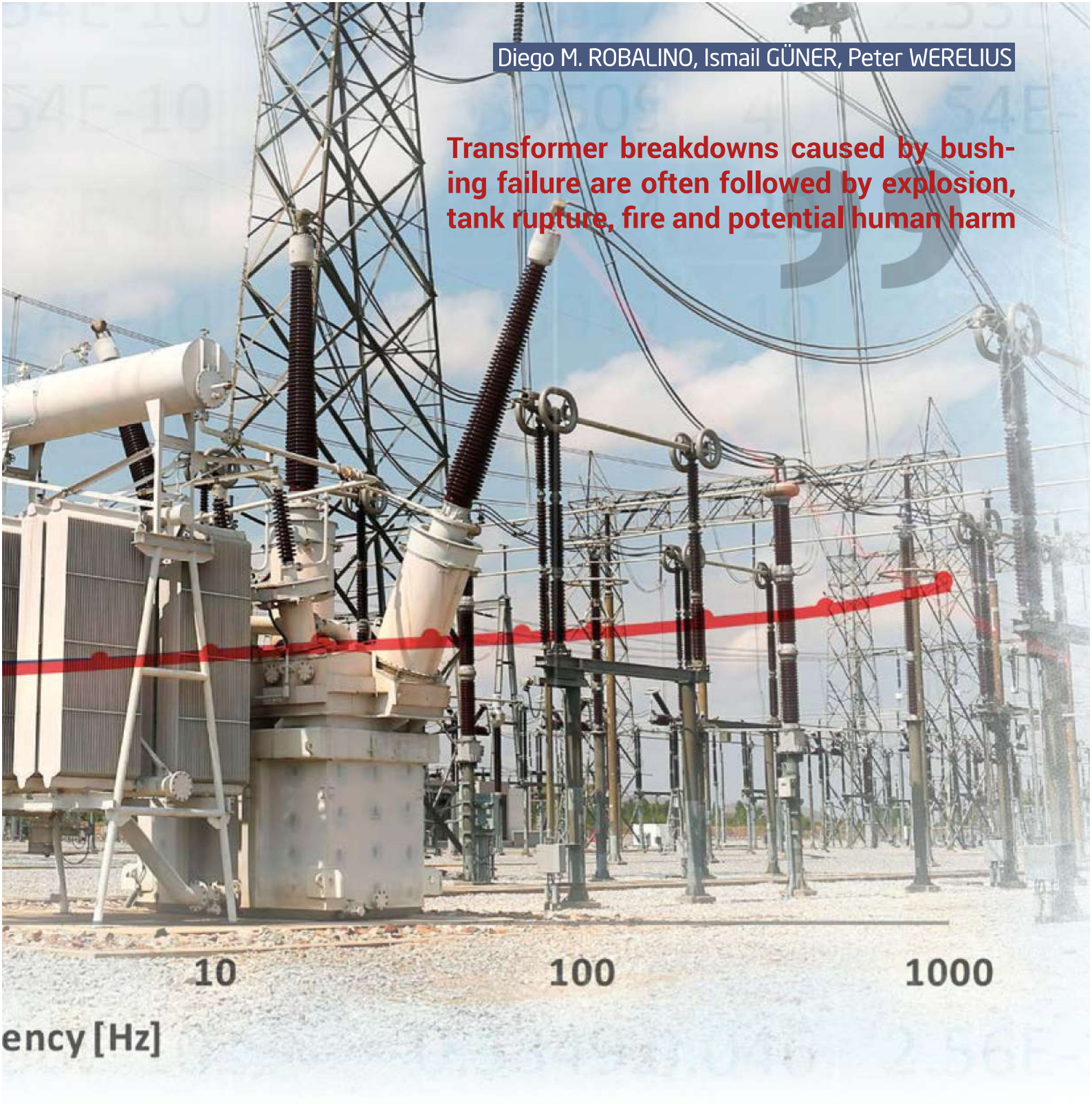

1. Introduction

The continuous growth in power demand and the need to maintain the highest levels of quality and reliability in the electrical power network enforce asset management teams to examine and pursue testing strategies to minimize the risk of operational down time.

Proper trending of the condition of high voltage (HV) and extra-high voltage (EHV) bushings is a priority. CIGRE TB 642 [1] reports approximately 17 % of transformer breakdowns caused by bushing failure are often followed by explosion, tank rupture, fire and potential human harm. It is of paramount importance, therefore, to dedicate sufficient resources to find procedures and methodologies to be applied as part of the asset management strategy.

In this work, specialists investigated different dielectric diagnostic methods capable to provide significant information to warn of potential risk of failure of EHV oil-impregnated paper (OIP) bushings. Data from power factor/dissipation factor (PF/DF), capacitance (C), HV Dielectric Frequency Response (DFR) measurements and Dissolved Gas Analysis (DGA) are considered collectively to establish potential correlation and guidelines for end users.

2. Bushing insulation – Routine testing practices

2.1. Power factor / Dissipation factor and capacitance test

The insulation design of HV and EHV bushings is a series of concentric layers made of conductive material with one layer made accessible for testing purposes at an external tap referred to as the test tap.

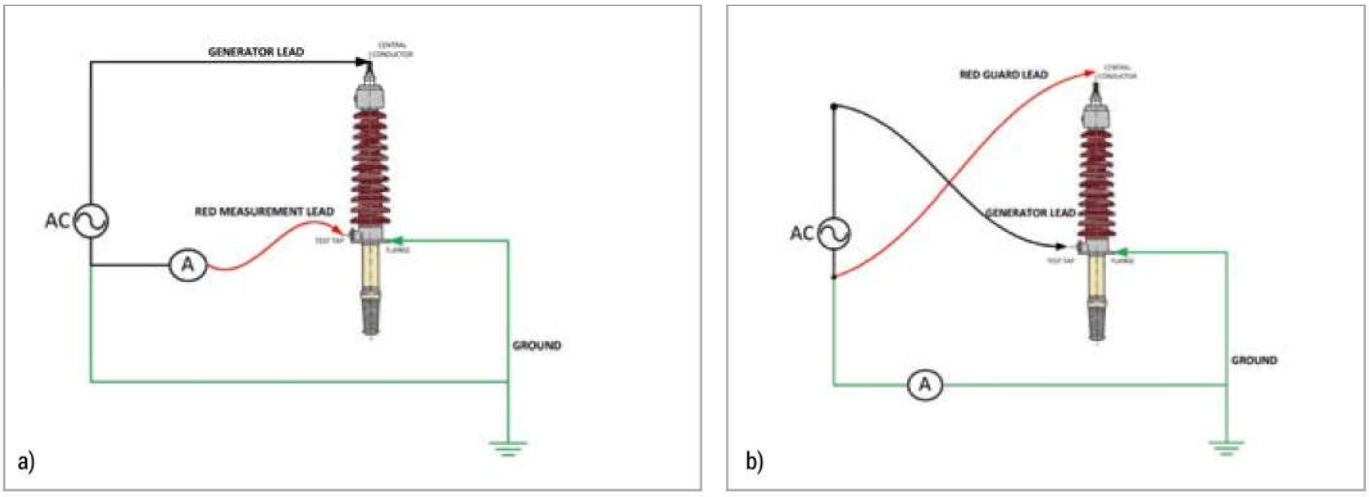

Figure 1. OIP EHV bushing, power factor / dissipation factor and Dielectric Frequency Response hook up diagram: a) Test on C_1 capacitance (UST mode); b) Test on C_2 capacitance (GSTg mode)

Through this test tap, main core insulation of the bushing is divided into two sub-capacitances: C_1 representing the insulation between the HV conductor and the test layer; and, C_2 representing the insulation between the test layer and the flange or ground when mounted on the transformer [2]. The test tap facilitates the execution of tests such as DFR, including PF/DF and capacitance of C_1 and C_2 as presented in Figure 1.

In the field, the value of C_1 capacitance and PF/DF can be tested and compared against the information on the bushing's nameplate. C_1 capacitance is tested under a UST (Ungrounded Specimen Test) mode. C_2 capacitance, as it is the measurement between the test and the flange intrinsically connected to ground through the tank of the transformer, is tested under a GSTg (Grounded Specimen Test with guard) mode. Bushing insulation PF/DF is typically a very low value because, among other reasons, it is generally processed to a greater degree of dryness than transformer insulation [3].

Bushing insulation PF/DF and capacitance routine tests are carried out typically at 10 kV for C_1 and at 500 - 2000 V for C_2 (or at those voltages suggested by the manufacturer) and at approximately line frequency according to the application (50/60 Hz).

It is easier and better to visualize the PF/DF results as a function of time in a trending chart. Test results of HV bushings with identical nameplates and exposed to similar electrical, thermal and mechanical stresses are ideal for comparative analysis. Any bushing with continued power factor increase should be further investigated and is a candidate for removal from service. A deficiency might be evolving in the insulation system. As described in CIGRE TB 642 [1], some of the deficiencies observed in HV OIP bushings' insulation include insulating fluid leaks and moisture contamination. Moisture is not the only factor leading to (a) an increase of dielectric losses, (b) accelerated aging of the insulation, and (c) possible failure of the HV bushing. Excessive partial discharge activity, accelerated thermal aging, contamination or degradation of the solid or liquid insulation may also result in increased dielectric loss and thus in increased PF/DF values.

Bushing insulation dissipation factor is typically very low because it is generally processed to a greater degree of dryness than transformer insulation

Take into account that PF/DF testing is not only frequency dependent but also temperature dependent. For factual trending analysis, the PF/DF factors obtained in the field should be corrected or normalized to 20 °C. Temperature correction factors provided by bushing manufactur-

Table 1. International standards' C1, PF/DF acceptance limits

Reference	Rated voltage	Test voltage	Maximum acceptance PF/DF value (%)	Temperature range °C	Factory	Field
IEC 60137	≥52 kV	$\frac{1.05 \cdot U_m}{\sqrt{3}}$ and U_m	0,7	10 to 40	X	
IEEE C57.19.01	≥69 kV	Typically 10 kV for C_1	0,5	Corrected to 20 °C	X	
IEEE C57.152	≥69 kV	Typically 10 kV for C_1	Rate of increase from 1.5 to 2 times initial reading	Corrected to 20 °C		X

ers and test equipment manufacturers are average at best and therefore may or may not match the true dielectric thermal condition of the HV apparatus at the time of testing. The use of Individual Temperature Correction (ITC) is advised for accurate PF/DF reference to 20 °C. Details of ITC as applied to PF/DF correction can be reviewed in the literature [4, 5].

PF/DF and capacitance tests on HV bushings for factory acceptance, commissioning and routine testing are recommended in technical brochures and international standards. Table 1 summarizes the acceptance limits indicated in the reference literature [6, 7, 8].

2.2. Dissolved Gas Analysis (DGA)

Under normal operation condition, thermal and electrical stress in OIP bushings produce low values of characteristic gases from the decomposition of solid and liquid insulation materials. The main causes of abnormal gas generation (high values of characteristic gases) in OIP HV bushings in service are thermal and electrical defects.

DGA has several methods used for interpretation of the concentration of hydrocarbon gases, including:

- Single gas analysis (Key gas method)
- Two gases at a time (Rogers, IEC method)
- Three gases (Duval Triangles)
- Most recent, five gases (Duval Pentagons)

The only reference found providing threshold values for key gases in HV OIP bushings is IEC TS 61464-1998 [9]. The threshold values given for hydrocarbon gases are outlined in Table 2.

If any of the gases exceeds the numbers listed in Table 2, an active fault condition may have developed, with possible fault conditions presented in Table 3.

IEC 61464 [9] provides significant ratios of gas concentrations and its relation to characteristic faults encountered in HV OIP bushings.

3. Dielectric Frequency Response

DFR is an advanced application of PF/DF testing. The DFR test set applies a sinusoidal excitation signal of low energy at the electrode on one end of the insulation system and measures the total current at the electrode on the other end of the insulation system under test, including the phase deviation between applied voltage and measured current.

The sinusoidal signal applied is of 140 Vrms and varies frequency in a wide spectrum, typically from 1000 Hz down to 1 mHz. As a result, a unique dielectric response curve displaying the correlation between capacitance, power factor or dissipation factor as a function of frequency is obtained.

In the field, testing of HV and especially EHV bushings with DFR is not a simple task. The information gathered from [10] describes the effect of electro-magnetic interference on time domain and frequency domain dielectric response measurements. The data shows that the dielectric response in the frequency domain is less susceptible to the effect of electromagnetic interference (EMI). Capacitance C_1 is typically very small (hundreds of pF)

Moisture, partial discharge, accelerated thermal aging, contamination or degradation of the solid or liquid insulation may result in increased dielectric loss

Table 2. OIP HV bushings DGA threshold

Type of gas	Concentration $\mu l_{gas}/l_{oil}$
H_2 – Hydrogen	140
CH_4 – Methane	40
C_2H_2 – Ethylene	30
C_2H_2 – Ethane	70
C_2H_2 – Acetylene	2
CO – Carbon monoxide	1000
CO_2 – Carbon dioxide	3400

Table 3. Correlation between key gases and possible fault conditions

Key gas generated	Characteristic fault
H_2	Surface discharge
H_2; CH_4	Partial discharge
C_2H_2; C_2H_4	Discharge of high energy
H_2; C_2H_2	Discharge of low energy
C_2H_4; C_2H_6	Thermal fault in oil
CO; CO_2	Thermal fault in paper

Table 4. Correlation between gas ratios and possible fault conditions

Ratio	Value	Characteristic fault
H_2 / CH_4	>13	Partial discharge
C_2H4 / C_2H_6	>1	Thermal fault in oil
C_2H2 / C_2H_4	>1	Discharges
CO_2 / CO	> 20 or <1	Thermal fault in paper

Main causes of abnormal gas generation in OIP HV bushings in service are thermal and electrical defects

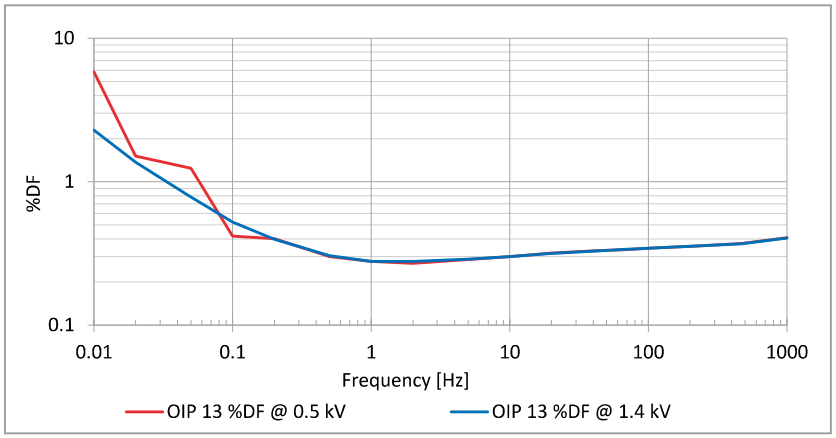

Figure 2. Dielectric response of an EHV OIP bushing measured in an operational 735 kV substation

The use of HV DFR at 1.4 kVrms allowed measurement of the dielectric response of EHV bushings in 735 kV substations and it is strongly recommended for this type of application

and therefore, the current measured at very low frequencies is very small and may be affected by DC or AC interference. For example, the capacitive current of a 365 pF capacitor measured at 10 mHz and 100 V becomes:

$$I_c = 2\pi f \cdot C \cdot V = 2\pi \cdot 0{,}01 \cdot 365 \cdot 10^{-12} \cdot 100 = 2.29\ nA \quad (1)$$

The only way to overcome such a measuring challenge is to run DFR at higher voltages to increase the signal-to-noise ratio (SNR) and be able to minimize the effect of noise on the dielectric response curves depicting the true condition of the EHV OIP bushing. Therefore, in the field and under high EMI, the use of a voltage booster is recommended. In Figure 2 the dielectric response of an EHV OIP bushing is obtained using a 0.5 kVrms signal and a 1.4 kVrms signal. The 1.4 kVrms provides a smooth response and useful information for analysis.

As observed in Figure 2, the paper insulation dominates the dielectric response and therefore, on EHV OIP bushings, measurements down to 10 mHz are sufficient for evaluation. Moreover, changes at 1, 0.1 and 0.01 Hz justify trending not just line frequency values, as concluded from the experimental work described next.

Figure 3. Shunt reactor with EHV OIP bushing

4. The experimental work

The asset management team embarked on a planned investigation to identify the root cause of failure in EHV OIP bushings mounted on shunt reactors at 735 kV power yards. High EMI and temperatures below 20 °C accompanied the testing procedure. A 735 kV shunt reactor with the EHV OIP bushing mounted is presented in Figure 3.

A total of 25 EHV OIP bushings were investigated using the following testing techniques:

- 10 kV PF/DF and capacitance at line frequency
- DGA
- Dielectric Frequency Response (1 kHz down to 10 mHz) at 1.4 kVrms

The data was carefully collected, threshold values were set based on reference standards listed previously, and the units with questionable values were singled out for comparative analysis.

From the PF/DF test at 10 kV and at line frequency, the numbers did not provide relevant distinction nor deviation from acceptable limits, as presented in Figure 4.

As observed in Figure 4, there is almost no deviation of field tested capacitance and certainly no increase of PF/DF at 60 Hz values properly corrected to 20 °C. It was interesting to observe values of PF with deviation below 20 % from the nameplate data. The decrease in PF is under investigation.

To the contrary, the dielectric response test provided clear differentiation between tested units, as presented in Table 5.

The data analyzed identifies clear deviation of the dielectric response at lower frequencies, namely 10 Hz and 1 Hz. Based on this information, a chart with all results properly corrected to a normalized temperature (20 °C) can be observed and color-coded accordingly.

The values obtained from DFR testing at different temperatures and at different frequencies were normalized to 20 °C using Individual Temperature Correction (ITC) algorithm and summarized in Figure 5.

Now, the data can be grouped in blocks of ideal, good and questionable condition. The units in the chart outside of these blocks are further investigated against DGA values to identify potential correlation. Table 6 summarizes the findings.

From Table 6, two units were selected for physical investigation (OIP 2 and OIP 19). Four key gases showed abnormal values and the dielectric response at 1 Hz was significantly higher than the other 22 units. The units were carefully disassembled and their gradient capacitance of each layer was tested. The bushing dissection revealed the presence of X-wax on the most inner layer of the insulation system. Unit OIP 17 did present abnormal concentration of C_2H_2 but no deviations in the DFR tests. OIP 17 is under observation.

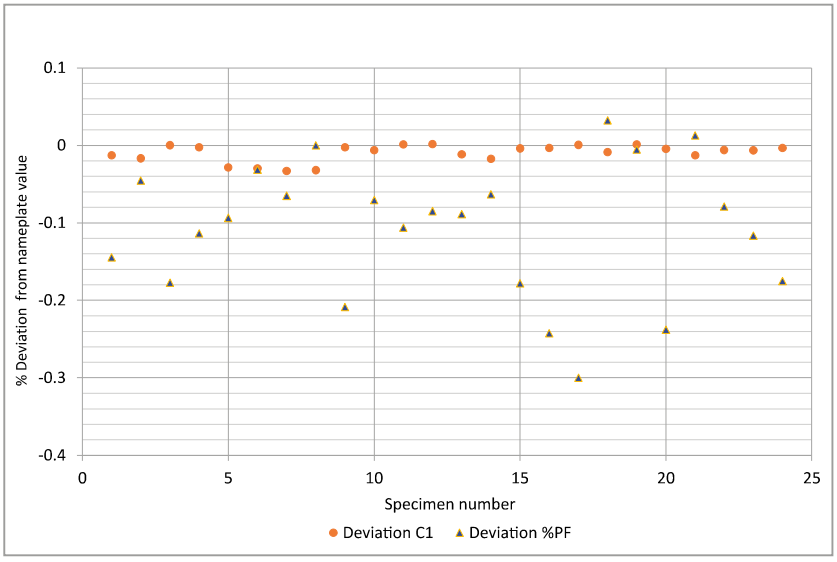

Figure 4. Percentage deviation from nameplate data; %PF and capacitance of C_1 for 24 specimens

The DFR data was converted into the DTR following the ITC principles and it was possible to confirm the differences in the thermal behavior of frequency PF/DF values at different temperatures

As presented here, a well-planned and carefully executed investigation was able to distinguish units with potential risk of failure and to determine the root cause of excessive concentration of key gases in the DGA results as well as deviation in the 10 Hz and 1 Hz PF/DF values obtained from DFR test.

Based on these results, the dielectric frequency response data was converted into the dielectric thermal response following the ITC principles and it was possible to confirm the differences in the thermal behavior of line frequency PF/DF values at different temperatures. The analysis confirms the condition evaluation of the EHV bushings in the frequency domain or in

Table 5. Dielectric Frequency Response on EHV OIP bushings

DFR	Specimen	Condition	%DF @ 20 °C			
			60 Hz	10 Hz	1 Hz	0.1 Hz
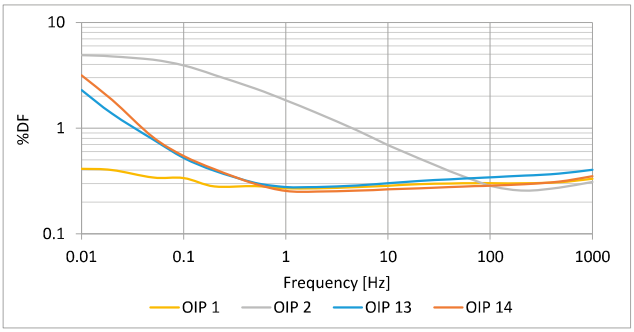	OIP 1	good	0,3	0,29	0,27	0,32
	OIP 2	bad	0,31	0,61	1,58	3,57
	OIP 13	good	0,32	0,29	0,28	0,57
	OIP 14	good	0,28	0,26	0,25	0,73

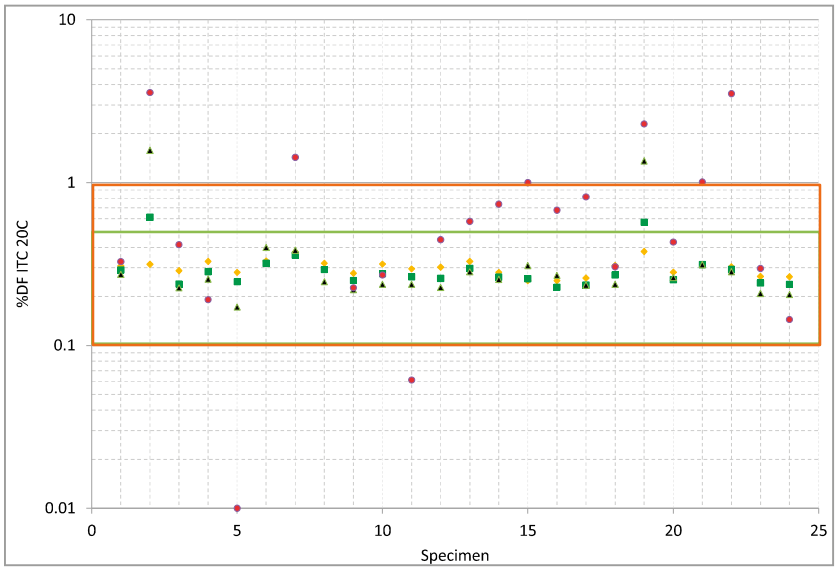

Figure 5. Ranking values for %PF/DF values at different frequencies

The application of the ITC algorithm supports another approach for analysis of the condition of the insulation, moving from the DFR to the DTR

Table 6. DFR and DGA threshold correlation

Sample	DFR threshold		DGA Threshold						
	1Hz	0.1Hz	H_2	CO	CO_2	C_2H_2	CH_4	C_2H_6	C_2H_4
OIP 2	X	X	X			X	X	X	
OIP 5		X							
OIP 6		X							
OIP 7		X							
OIP 8		X							
OIP 11		X							
OIP 17						X			
OIP 19	X	X	X			X	X	X	
OIP 21		X							
OIP 22		X							

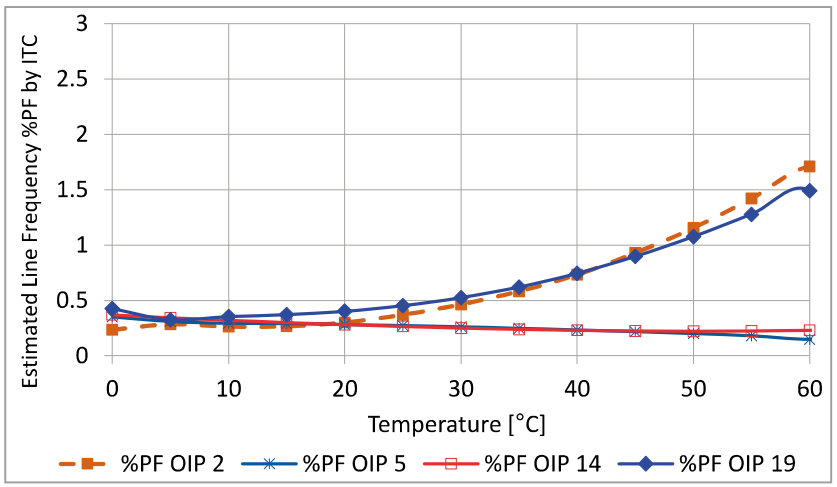

Figure 7. Dielectric thermal response (DTR) of EHV OIP bushings

Figure 6. X-wax found on the most-inner layer of the EHV bushing disected

the "temperature" domain, as presented in Figure 7.

The conversion from DFR into DTR using the individual temperature correction (ITC) algorithm was previously published in Transformers Magazine [4]. The Dielectric Thermal Response (DTR) becomes another tool for condition analysis of the insulation system based on the thermal response of PF/DF properly converted to a wide range of temperatures between 5 and 60 °C. The data suggests establishing PF/DF temperature indicators at 40 and 50 °C. Correlation with DGA analysis is carried out and summarized in Table 7.

Conclusions

The assessment of capacitance and DF/PF measurements normalized to 20 °C and at line frequency was not conclusive. The analysis of the dielectric response corrected to 40 and 50 °C differentiated the response from other units in this project. Therefore, the application of the Individual Temperature Correction (ITC) algorithm supports another approach for analysis of the condition of the insulation moving from the Dielectric Frequency Response to the Dielectric Thermal Response.

Because of the low capacitance and the low frequencies used to obtain the dielectric response of the C_1 capacitance

in the EHV OIP bushings, the low current measurement may be affected by the EMI in the substation. The use of HV DFR at 1.4 kVrms allowed measurement of the dielectric response of EHV bushings in 735 kV substations and it is strongly recommended for this type of application.

DGA, DFR and DTR identified OIP 2 and OIP 19 to be defective. The specific case of OIP 17 is under observation. In OIP 2 and OIP 19, four key gases presented abnormal values and DFR observed elevated values at 1 Hz. In the analysis of OIP 17, only one key gas showed higher values of C_2H_2, but no other gas has indicated any reason for concern, neither did DFR. OIP 17 is under observation.

The experimental work and the dissection carried out on the specimens determined that DFR technique can be used to detect the presence of solid particles of carbon and hydrocarbon polymers (X-wax).

HV DFR in conjunction with DGA and routine testing provide a strong support for asset managers, operations and maintenance staff to decide if the EHV bushing may be considered a potential risk to the operation.

Table 7. Correlation between DTR and DGA

Sample	Indicator Thermal Response		Indicator DGA						
	40 °C	50 °C	H_2	CO	CO_2	C_2H_2	CH_4	C_2H_6	C_2H_4
OIP 2	X	X	X			X	X	X	
OIP 17						X			
OIP 19	X	X	X			X	X	X	

References

[1] CIGRE TB 642, *Transformer Reliability Survey*, WG A2.37. 2015

[2] CIGRE TB 445, *Guide for Transformer Maintenance*, WG A2.34. 2011

[3] IEEE C57.19.100, *Guide for the Application of Power Apparatus Bushings,* 2012

[4] D. Robalino, *Individual temperature compensation – Benefits of dielectric response measurements*, Transformer Magazine, Vol. 2, Issue 3. July 2015, pp. 42 – 47

[5] D. Robalino, *Accurate temperature Correction of Dissipation Factor data for Oil-impregnated Paper insulation Bushings: Field Experience*, Proceedings of the IEEE CEIDP, 2011

[6] IEC 60137, *Insulated bushings for alternating voltages above 1000 V*, fifth edition, 2003-08

[7] IEEE C57.152, *Guide for Diagnostic Field Testing of Fluid-Filled Power Transformers, Regulators, and Reactors*, 2013

[8] IEEE C57.19.00, *Standard General Requirements and Test Procedures for Power Apparatus Bushings,* NY, 2005

[9] IEC TS 61464:1998, *Insulated bushings - Guide for the interpretation of dissolved gas analysis (DGA) in bushings where oil is the impregnating medium of the main insulation*

[10] P. Werelius, M. Ohlen, J. Skoldin, *Dielectric Frequency Response Measurement Technology for Measurements in High Interference AC and HVDC Substations,* TechCon Asia Pacific, 2011

Authors

Diego Robalino currently works for Megger as Principal Engineer, where he specializes in the diagnosis of complex electrical testing procedures. While doing research in power system optimization with a focus on aging equipment at Tennessee Technological University, Robalino received his electrical engineering Ph.D. from that institution. Robalino has over 20 years of involvement in the electrical engineering profession with management responsibilities in the power systems, oil and gas, and research arenas. Dr. Robalino is a Senior Member of the IEEE, member of the IEEE transformers main committee and a Certified Project Management Professional with the PMI.

Ismail Güner received the B.E. degree in electrical engineering from École Polytechnique de Montréal, Canada. He worked as an electrical design engineer in large power transformers industry. He currently holds the position of transformer asset management engineer at Hydro-Québec. He is an active member of IEEE transformers committee working groups.

Peter Werelius received his Ph.D. in electrical engineering from KTH Royal Institute of Technology, Sweden, developing the Dielectric Frequency Response (DFR) technique for diagnosis of medium voltage XLPE cables. Peter began his professional career starting up a spin-off company, WaBtech, in 1996, manufacturing the first field DFR test equipment. Peter improved and further developed DFR technology and its applications under WaBtech, Programma, GE, Pax Diagnostics and now Megger. Peter works for Megger Sweden as an applications and product specialist with responsibilities related to research, product development, product sustainability and training for the Megger Global organization. Dr. Werelius is a member of SEK TC14, IEEE and CIGRE and actively participates in working groups and task forces, especially those related to FDS/DFR and SFRA. Throughout his career, he has participated in relevant technical conferences, authored technical papers and patents.